such as acetonitrile, Pth can be successfully deposited on platinum only from a relatively concentrated monomer solution. On the contrary, in freshly distilled BFEE, the monomer concentration may be as low as 2 mM. Indeed, high-quality Pth films were obtained only by ensuring that the monomer concentration was lower than 10 mM. The Pth film with the highest quality was obtainable only with the use of freshly distilled BFEE (with a monomer concentration lower than 10 mM) as the electrolyte and stainless steel as the substrate and at an applied potential of 1.3 V (versus Ag/AgCl). The film prepared at this condition was shiny and metal-like, and its strength was greater than that of aluminum and it could be cut into a variety of structures with mechanical methods.

REFERENCES AND NOTES

1. G. Tourillon and F. Garnier, *J. Electroanal. Chem.* **135**, 173 (1982).
2. T. Yamamoto, H. Wakayama, F. Takahashi, K. Takaki, *J. Phys. Chem.* **96**, 8677 (1992).
3. A. J. Downard and D. Pletcer, *J. Electroanal. Chem.* **206**, 147 (1986).
4. G. Tourillon and F. Garnier, *J. Phys. Chem.* **87**, 2289 (1983).
5. M. Salmon, A. F. Diaz, A. J. Logan, M. Kronbi, J. Bargon, *Mol. Cryst. Liq. Cryst.* **83**, 1297 (1982).
6. A. G. McDiarmid, L. S. Yang, W. S. Huang, B. D. Humphrey, *Synth. Met.* **18**, 393 (1987).
7. P. J. Nigrey, A. G. McDiarmid, A. J. Heeger, *J. Chem. Soc. Chem. Commun.* **1979**, 594 (1979).
8. T. Nakajima and T. Kawagoe, *Synth. Met.* **28**, C629 (1989).
9. H. Yoneyama, H. Wakomoto, H. Tamura, *J. Electrochem. Soc.* **132**, 2414 (1985).
10. E. W. Panl, A. J. Ricco, M. S. Wrighton, *J. Phys. Chem.* **89**, 1441 (1985).
11. A. Tsumura, H. Koezuka, S. Tsunoda, T. Ando, *Chem. Lett.* **1986**, 683 (1986).
12. W. H. Heyer, H. Kiess, B. Bingelli, E. Meier, G. Harbeke, *Synth. Met.* **10**, 255 (1985).
13. H.-L. Wang and J. E. Fernandez, *Macromolecules* **25**, 6179 (1992).
14. S. Li, C. W. Macosko, H. S. White, *Science* **259**, 957 (1993).
15. Y. Zhang and D. A. Shores, *J. Electrochem. Soc.* **141**, 1255 (1994).
16. R. R. Gagne, J. L. Allison, R. S. Call, C. A. Coval, *J. Am. Chem. Soc.* **99**, 7170 (1977).
17. R. M. Eales and A. R. Hillman, *J. Electroanal. Chem.* **250**, 219 (1988).
18. M. Gratzl, D.-F. Hsu, A. M. Riley, J. Janata, *J. Phys. Chem.* **94**, 5973 (1990).
19. B. Kritsche and M. Zagorska, *Synth. Met.* **28**, C263 (1989).
20. K. Tanaka, T. Shichiri, S. Wang, T. Yamabe, *ibid.* **24**, 203 (1988).
21. G. Tourillon and F. Garnier, *J. Electroanal. Chem.* **161**, 407 (1984).
22. D. Ofer, R. M. Crooks, M. S. Wrighton, *J. Am. Chem. Soc.* **112**, 7869 (1990).
23. C. Chorro, B. Moukala, J.-P. Leer-Porte, J. Petrissans, *Mol. Cryst. Liq. Cryst.* **187**, 199 (1990).
24. R. J. Waltman, J. Margon, A. F. Diaz, *J. Phys. Chem.* **87**, 1459 (1987).
25. G. Grecelius, M. Stamm, J. Fink, J. Ritsko, *Phys. Rev. Lett.* **50**, 1498 (1983).

26. This work was supported by the research foundation of the national key laboratory of coordination chemistry of Nanjing University.

15 August 1994; accepted 23 November 1994

Simultaneous Studies of Reaction Kinetics and Structure Development in Polymer Processing

W. Bras, G. E. Derbyshire, D. Bogg, J. Cooke, M. J. Elwell, B. U. Komanschek, S. Naylor, A. J. Ryan*

The simultaneous time-resolved study of structure development and reaction kinetics during polymer processing is an experimental method that has great potential in developing a deeper understanding of the parameters that govern the formation of structure and therefore polymer properties. A combination of synchrotron radiation small-angle x-ray scattering and Fourier-transform infrared spectroscopy experiments have been performed on a series of model segmented block copolyurethanes. These studies confirm that the driving force for structure development in polyurethanes is the thermodynamics of phase separation rather than hydrogen bonding.

One significant advantage of using synchrotron radiation small-angle x-ray scattering (SAXS) beam lines for polymer processing studies is that the high x-ray intensity allows time-resolved x-ray scattering experiments on polymers to be performed with a resolution comparable to the time scales used in the processing of such polymers. This provides a useful insight into the morphological changes that take place in the materials during processing.

When time-resolved SAXS experiments are done simultaneously with additional experimental techniques, a wealth of information can be derived from a single sample, and the artifacts introduced by the combination of two independent experiments are avoided (that is, temperature- or thermal-history differences and inaccuracies in the time correlations between the experiments). Successful experiments using the concept of combined techniques have been reported in recent years. The SAXS technique, wide-angle x-ray scattering, and differential scanning calorimetry have all been combined in a single experiment (*1*, *2*), and so has light scattering and SAXS (*3*).

For the reactive processing of polymers (that is, all thermosetting materials), understanding of the development of structure and properties during polymerization requires a transformation of data from the (experimental) time domain into the (molecular) conversion domain because many processes involve a chemical quench from the one-phase region to the two-phase region of a ternary phase diagram. In the conversion domain, the evolution of structure may be related to the increase of molecular weight, which locates a material in a phase diagram independently of reaction kinetics.

Fourier-transform infrared spectroscopy (FTIR) is a widely used tool in the characterization of polymers (*4*), especially for following the reaction kinetics and phase-separation dynamics during reaction-induced phase transformations (*5*). The FTIR technique has proven most successful in the special case of segmented urethane block copolymers, where the soft and hard block sequences can undergo microphase separation and subsequent hydrogen bonding. The technique is used to determine the chemical reaction kinetics from the decrease in the isocyanate absorbance and to find the hydrogen bonding dynamics from the subtleties of the carbonyl absorbances (*6*–*9*). In most reports (*6*–*9*), determination of hydrogen bonding has been associated with the onset of phase separation. Independent SAXS studies attempting to reproduce the FTIR conditions (*10*) indicate that microphase separation determined directly by SAXS may precede hydrogen bonding. However, the difference in conversion between the phase separation and hydrogen bonding, as probed by the two independent techniques, is at the limit of the error between experiments, ~2%. Whether microphase separation precedes hydrogen bonding is of fundamental scientific and technological importance in the processing of polyurethane materials (the annual market is 10^7 metric tons per year). The combination of time-resolved FTIR with x-ray scattering techniques is therefore an excellent tool for the study of these phase transitions, providing a correlation between reaction kinetics and structure development or other morphological changes.

We have developed equipment that al-

W. Bras, Netherlands Organization for Scientific Research (NWO) and Daresbury Laboratory, Warrington WA4 4AD, UK.
G. E. Derbyshire, D. Bogg, B. U. Komanschek, Daresbury Laboratory, Warrington WA4 4AD, UK.
J. Cooke, M. J. Elwell, S. Naylor, Manchester Materials Science Centre, University of Manchester Institute of Science and Technology, Manchester M1 7HS, UK.
A. J. Ryan, Manchester Materials Science Centre, University of Manchester Institute of Science and Technology, Grosvenor Street, Manchester M1 7HS, and Daresbury Laboratory, Warrington WA4 4AD, UK.
*To whom correspondence should be addressed.

lows the FTIR and SAXS experiments to be performed simultaneously. Sample thickness is an important factor: The optimum sample thicknesses for the FTIR experiment (<30 μm) and the SAXS experiment (~1.5 mm) are incompatible. This difference makes it difficult to perform both experiments in the transmission geometry unless one is prepared to accept very poor signal-to-noise ratios in the scattering experiments. A solution is to perform the SAXS experiment in transmission and use the attenuated total reflection (ATR) method for the FTIR experiment (*4*).

The experiments have been performed at SAXS station 8.2 at the Synchrotron Radiation Source (Daresbury, United Kingdom). An extensive description of this experimental facility is given elsewhere (*2*). In essence, the station produces a high-intensity, well-collimated x-ray beam with a fixed wavelength of $\lambda = 1.5$ Å. A Nicolet 5 DX Infrared Spectrometer was adapted to provide x-ray access to the sample chamber. A special backing plate for the sample stage was constructed (Fig. 1) that allowed a Kapton (Dupont) embedded heater element to be inserted between the sample and the ATR crystal. Care was taken to match the heat capacity of the mounting plate at the x-ray access window to that of the ATR crystal to avoid temperature differences. Thermocouples were mounted at several positions and showed a discrepancy of ±3°C between the sample temperature at the point of x-ray access and that at the IR position for temperatures above 100°C. The sample was a single uniform film of material sandwiched between the mounting plates and the crystal.

The experiment we report involves a chemical reaction that results in the formation of a diblock copolymer and some homopolymer from a mixture of monomers. The chemistry and microstructure formed are illustrated in Fig. 2; the complete chemical details will be published elsewhere (*11*). The hard block was formed from 4,4′-diphenyl methane diisocyanate (MDI) (Isonate M143 L; Dow) and an asymmetric diol, pentane-1,5-diol (Aldrich). The soft segment was a monofunctional poly(ethylene oxide)–tipped poly(propylene oxide) with a nominal molar mass of 2000 (equivalent weight of 1996 g mol^{-1} by end-group analysis). The hard block content was 31% by weight.

The monofunctional polyether and pentane diol were weighed, transferred to a mixing vessel, and stirred vigorously for 60 s. Preweighed MDI was then added, and the mixture was stirred for an additional 60 s. A small proportion of the reaction mixture (~0.5 cm^3) was transferred to the SAXS sampling environment, and the ATR crystal was coated with another ~0.5 cm^3 of the mixture. The SAXS and FTIR data acquisition were initiated simultaneously (*12*).

We collected IR spectra at a resolution of 2 cm^{-1}, co-adding 60 scans per file. The IR spectra for the background file were also obtained at 2-cm^{-1} resolution, co-adding 60 scans per file before the execution of a kinetic run. The SAXS data were collected in a series of time frames of 30 s each. The background theory and analysis of the spectroscopic data and the data analysis procedure for SAXS have been described in detail elsewhere (*10, 13, 14*).

The evolution of the SAXS profile as function of time is shown in Fig. 3. A

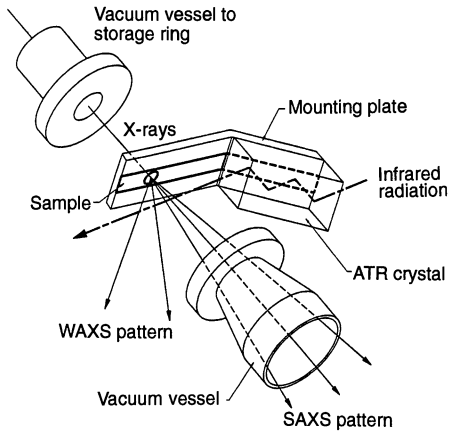

Fig. 1. The sample position of the combined SAXS-FTIR equipment. The x-ray beam (measuring 0.3 mm by 3 mm) impinges onto the sample. The x-ray scattering pattern falls onto the position-sensitive detector. Between the sample and the detector, a vacuum chamber is inserted to reduce air scatter and absorption. The IR radiation bounces several times through the ATR crystal, which is on one side in close contact with the reacting material. WAXS, wide-angle x-ray scattering.

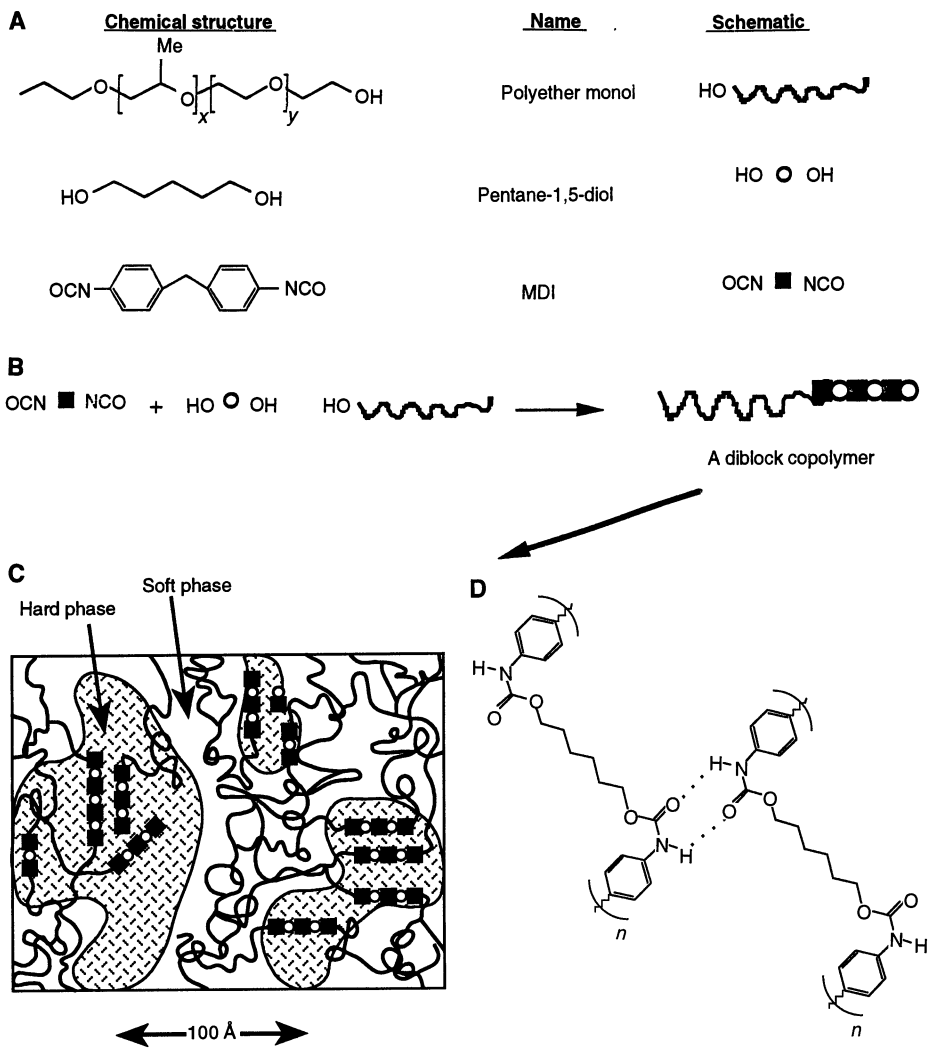

Fig. 2. (**A**) The chemical structures and names of the reactants; Me, methyl. (**B**) Schematic of their reaction to form a block copolymer; the monofunctional polyether forms a flexible polyether block, and the MDI and pentane-1,5-diol combine to form a rigid (hard) polyurethane block. (**C**) Microphase separation into a dispersed hard phase and a continuous soft phase, with an approximate dimension of 100 Å. (**D**) The orientation of the urethane sequences (hard block domain) to form intermolecular hydrogen bonds.

diffraction peak at $q = 0.05$ Å^{-1} grows in time. This peak indicates that a structure is formed with a spacing of ~118 Å. The polymerization causes a quench from the disordered to the ordered state of the phase diagram because of the increase in molecular weight during the reaction.

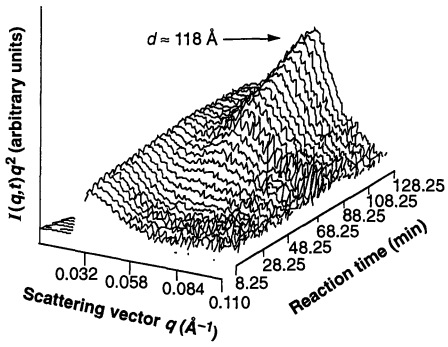

Fig. 3. The time evolution of the SAXS pattern is shown as a time-stack of the Lorentz-corrected diffraction intensity (Iq^2) versus scattering vector [$q = (4\pi/\lambda)\sin(\theta/2)$, where θ is the scattering angle]. The scattering pattern from an oriented specimen of wet collagen (rat tail tendon) was used to calibrate the SAXS detector. Parallel plate ionization detectors placed before and after the sample cell recorded the incident and transmitted intensities. The experimental data were recorded in frames of 30 s and were corrected for background scattering (subtraction of the scattering from the camera and an empty cell), sample thickness and transmission, and the positional alinearity of the detectors. For clarity, only every fourth frame of data is shown. Initially, there is little scattering, and the peak that starts to grow at $q^* = 0.053$ Å^{-1} after ~40 min is evidence for the structural development in the sample with a linear dimension of ~118 Å. Block copolymer theory (*15*) predicts that $2 \leq q^*R_g \leq 3$, where q^* is the SAXS peak position and R_g is the radius of gyration of the molecule (~60 Å).

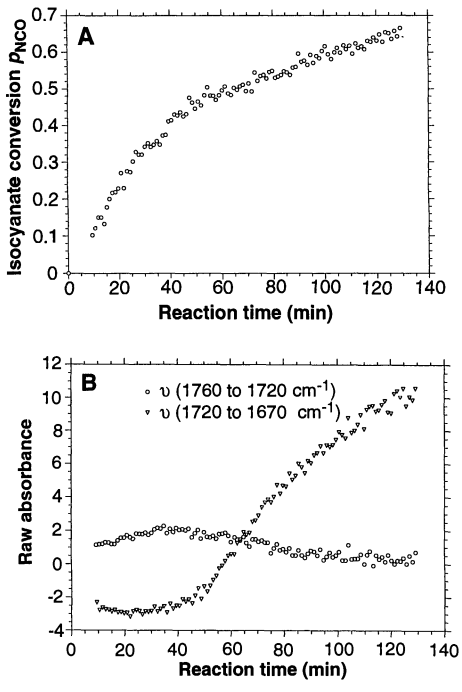

Fig. 4. (**A**) The reaction kinetics are determined in terms of the isocyanate conversion. The change in the absorbance of the isocyanate at 2300 cm^{-1} is normalized by an absorbance that is not affected by the reaction, such as a CH_2 stretch, to account for changes in crystal wetting and absorption. The extent of reaction, p_{NCO}, may be calculated from $p = 1 - (A_t/A_0)$, where A_t is the isocyanate absorbance at time t. The initial portion of the curve ($0 < t < 50$ min) follows second-order kinetics, as is commonly observed for urethanes (*5*), and at longer times, the reaction becomes diffusion controlled and conversion is linear in time. The transition from second-order kinetics to diffusion control occurs at $p \approx 0.45$ and is associated with a phase transition. (**B**) The state of association and hydrogen-bond dynamics are probed by the carbonyl absorbances in the range 1760 to 1670 cm^{-1}. The raw integrated absorbances are plotted against time. The free urethane at ~1740 cm^{-1} initially increases as urethane is created by the reaction of isocyanate and hydroxyl, and after ~50 min, the free urethane signal starts to fall and there is a concomitant growth in the hydrogen-bonded carbonyl at ~1700 cm^{-1}. The change from free to hydrogen-bonded carbonyl has been associated with the microphase separation transition (*6–10*).

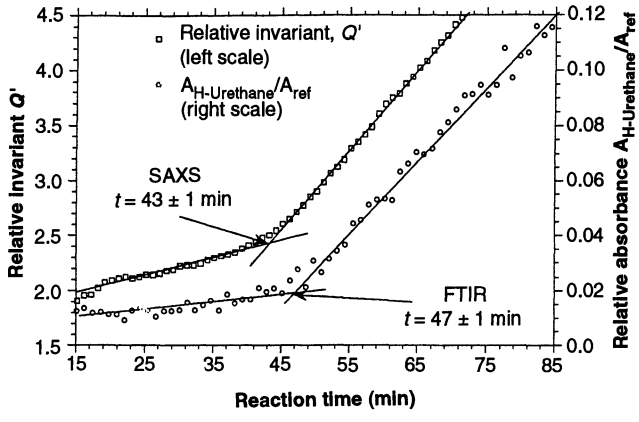

Fig. 5. The SAXS relative invariant Q' (*16*) and the normalized FTIR absorbance associated with hydrogen-bonded urethane are plotted against time. Tangents have been fitted to both data sets in order to estimate the onset time for microphase separation (t_Φ) and hydrogen bonding (t_H). The values of t_Φ and t_H are 43 ± 1 and 47 ± 1 min, respectively. The perfect time correlation between the two techniques confirms that microphase separation precedes hydrogen bonding in the reactive processing of this polyurethane block copolymer.

The time evolution of the FTIR signals is given in Fig. 4. The depletion of the absorption at 2300 cm^{-1}, which is associated with the isocyanate group, is used to calculate the conversion of isocyanate into urethane, and from this, the molecular weight and sequence length distribution can be predicted (*5*). The reaction shows second-order kinetics for the first 50 min, and at longer times, it becomes diffusion-controlled. The loss of the isocyanate peak is accompanied by a growth in urethane carbonyl absorption. The polymerization reaction is characterized by an initial increase in the amount of free urethane (with a carbonyl absorption at ~1740 cm^{-1}). After 50 min, the carbonyl absorption associated with free urethane reaches a maximum and then decreases. Coincident with this decrease is a sharp increase in the hydrogen-bonded urethane associated with the carbonyl absorption (absorption energy, ~1700 cm^{-1}).

Data with a perfect time-correlation between the microphase state, from the SAXS invariant, and hydrogen bonding, from the FTIR carbonyl absorbances, gives an insight into the structuring process during this block copolymer–forming reaction. For SAXS, we calculate the scattering power or invariant by integrating the area under the Iq^2 curve (where I is the intensity of the signal and q is the scattering vector), and for the FTIR, we divide the integrated carbonyl absorption-associated hydrogen-bonded urethane by the conversion so as to maintain a constant probe intensity. We estimated the onset of the phase transition for both techniques by tangent extrapolation (Fig. 5). That microphase separation precedes hydrogen-bond formation is now in no doubt: The time difference of 4 min in the onset of the transitions is readily resolved by this combined instrument. The result is interpreted as the thermodynamics of phase separation dominating the kinetics of hydrogen bonding. Phase separation is driven by the free energy of mixing and causes the hydrogen-bondable groups to achieve a locally high concentration; thus, their rate of association increases. We can draw a simple analogy in terms of polyurethane structure and properties. The microphase separation process closes the door on defining the structure; the hydrogen bonds turn the key and locks in the structure.

The implications of these data for experimental polymer science are significant. Two phase systems that can hydrogen-bond are not necessarily in a single phase if no hydrogen bonds can be detected; put another way, a strongly ordered system may result before the development of a hydrogen-bonded structure. The FTIR technique should not be used as a tool for studying

phase transitions without some other check on the phase structure of the materials in question; this caveat obviously applies to biological and food scientists also.

REFERENCES AND NOTES

1. T. P. Russell and J. T. Koberstein, *J. Polym. Sci.* **23**, 1109 (1985).
2. W. Bras *et al.*, *J. Phys. IV (Paris)* **3** (no. 8), 447 (1993).
3. M. Bark, C. Schulze, H. Zachmann, *Polym. Prepr. Am. Chem. Soc. Div. Polym. Sci.* **31** (no. 2), 106 (1990).
4. J. L. Koenig, *Spectroscopy of Polymers* (ACS Reference Book, American Chemical Society, Washington, DC, 1992).
5. C. W. Macosko, *RIM: Fundamentals of Reaction Injection Molding* (Hanser, Munich, 1988).
6. H. S. Lee and S. L. Hsu, *Macromolecules* **22**, 1100 (1989).
7. R. D. Priester Jr. *et al.*, *J. Cell. Plast.* **26** 346, (1990).
8. W. P. Yang and C. W. Macosko, *Makromol. Chem. Macromol. Symp.* **25**, 23 (1989).
9. H. S. Lee, Y. K. Wang, W. J. MacKnight, S. L. Hsu, *Macromolecules* **21**, 270 (1988).
10. M. J. E. Elwell, thesis, University of Manchester (1993).
11. A. J. Ryan, M. J. E. Elwell, G. E. Derbyshire, D. Bogg, W. Bras, in preparation.
12. The FTIR and SAXS data acquisition systems were controlled by separate computers. The 1-min time resolution allowed a manual start of both systems without the introduction of a significant error.
13. M. J. E. Elwell, A. J. Ryan, H. J. M. Grünbauer, H. C. van Lieshout, J. A. Thoen, *Prog. Rubber Plast. Technol.* **9**, 120 (1993).
14. A. J. Ryan *et al.*, *Macromolecules* **24**, 2883 (1991).
15. F. S. Bates and G. H. Fredrickson, *Annu. Rev. Phys. Chem.* **41**, 525 (1990).
16. The SAXS relative invariant is

$$Q' = \int_{0.01}^{0.20} I(q,t)q^2 dq$$

where I is the intensity of the signal, q is the scattering vector, and t is time.

17. The Engineering and Physical Sciences Research Council (EPSRC) is acknowledged for x-ray beam time. D. Bouch and P. Hindley provided valuable technical support. Reagents were supplied by and M.J.E. was supported by Dow Chemicals. J.C. and S.N. were supported by EPSRC studentships.

11 August 1994; accepted 6 December 1994

Evidence from Ion Chromatography Experiments That Met-Cars Are Hollow Cage Clusters

Seonghoon Lee, Nigel G. Gotts, Gert von Helden, Michael T. Bowers*

Ion chromatography studies were performed to assess various models proposed for the structure of M_8C_{12} species, the met-cars. A laser desorption source was used to make a sequence of titanium-carbon clusters centered around $Ti_8C_{12}^+$. The $Ti_8C_{12}^+$ was determined to be a hollow cage cluster, with the dodecahedron structure originally proposed giving the best fit to experiment; cubic structures could be excluded. Collisional breakup of $Ti_8C_{12}^+$ yielded only $Ti_7C_{12}^+$ under the experimental conditions described herein, and modeling indicated that the cage structure was retained. Both $Ti_8C_{11}^+$ and $Ti_8C_{13}^+$ were made by the cluster source, and again, dodecahedral-type cage structures were consistent with experiment. The extra carbon atom in $Ti_8C_{13}^+$ was attached exohedrally to a single titanium atom. No evidence for an endohedral species was found.

The discovery (*1*) and bulk synthesis (*2*) of fullerenes has allowed the structure of these hollow cage carbon clusters to be determined by traditional spectroscopic means (*3*). However, for all other larger ($n \geq 10$) carbon clusters, the most reliable and nearly exclusive structural evidence comes from ion chromatography (IC) studies (*4*, *5*). The IC studies showed that large, planar ring systems competed with fullerenes in the size range $n = 30$ to 60 (*4*–*8*) and in fact are the primary precursors of fullerenes formed in laser desorption sources (*8*–*10*).

In parallel development, Castleman and co-workers (*11*) discovered a class of stable metallo-carbon composites with the stoichiometry M_8C_{12}, where M was one of several transition metals. These species were identified by their "magic" character in mass spectra where, under certain source conditions, the mass-to-charge (m/z) peak corresponding to M_8C_{12} completely dominated neighboring species. Castleman proposed a dodecahedral cage structure of T_h symmetry composed of a cube of M atoms with C_2 units raised off each cube face and coined the term met-cars for these putative metallocarbohedrene species.

This proposition prompted a rapid response from the theoretical community, which rather quickly confirmed that M_8C_{12} cages were particularly stable species (*12*), although a somewhat lower energy was predicted for a distorted M_8 cube of T_d symmetry with the C_2 units rotated along the cube diagonals. This structure is composed of two tetrahedral pairs of four metal atoms rather than the eight equivalent atoms of the dodecahedral structure. Castleman and coworkers provided indirect evidence for a cage structure by showing that $Ti_8C_{12}^+$ would attach a maximum of eight polar ligands (H_2O, ND_3, and CH_3OH), indicating that all Ti centers were available for bonding (*13*). Only four π-type ligands could be attached (C_2H_4, C_6H_6), which could indicate that either steric hindrance is involved or four of the Ti atoms are more accessible than the remaining four. Subtle changes in the structure of the Ti_8C_{12} backbone could occur as a result of the attachment reactions.

We applied the IC technique (*14*, *15*) to both carbon cluster ions (*4*–*6*, *8*, *9*) and to small carbon-metal composite clusters (*16*). In conjunction with computer modeling, IC allows us to probe the shape of cluster ions by measuring their mobilities. We have shown that isomeric species that differ substantially in structure can be readily identified and many salient features about their structures unambiguously determined. The experimental setup has been described (*15*, *17*). Cluster cations were generated in a standard laser vaporization supersonic expansion source (*18*). Once inside the IC cell, the mass-selected pulse of ions was subjected to a small uniform electric field that gently drifted the ions through a bath of He gas, usually present at 3 to 5 torr (at 300 K). The ion packet eventually exited the cell, was mildly accelerated, and was passed through a quadrapole mass filter, and an arrival time distribution (ATD) was obtained at the detector. For a single geometric isomer of a single cluster ion, the ATD could be readily converted to an ionic mobility. If multiple isomeric structures were present, then the IC device would spatially and temporally separate them if they differed significantly in shape. In this case, the ATD would have several peaks. The detailed shape (that is, the width) of each individual peak could, if necessary, be accurately reproduced by using the transport characteristics of that ion through He gas.

A mass spectrum obtained under typical operating conditions is shown in Fig. 1A. The series of peaks are separated by 12 atomic mass units (amu), and the strong peak at 528 amu corresponds to the correct mass of a singly charged Ti_8C_{12} cluster. However, the 528-amu peak could possibly be C_{44}^+. A high-resolution spectrum (Fig. 1B) shows that the underlying isotopic distribution agrees within 1% of that expected for $Ti_8C_{12}^+$ and bears no resemblance to that expected for C_{44}^+. Similarly, the peaks centered near 516 and 540 amu can be shown to be $Ti_8C_{11}^+$ and $Ti_8C_{13}^+$, respectively.

Department of Chemistry, University of California, Santa Barbara, CA 93106, USA.

*To whom correspondence should be addressed.